P H Y S I C A L   R E V I E W   L E T T E R S

Equilibrium Capillary Forces with Atomic Force Microscopy

J. Sprakel,[*] N. A. M. Besseling, F. A. M. Leermakers, and M. A. Cohen Stuart

Laboratory of Physical Chemistry and Colloid Science, Wageningen University,
Dreijenplein 6, 6703 HB Wageningen, The Netherlands
(Received 27 March 2007; published 7 September 2007)

We present measurements of equilibrium forces resulting from capillary condensation. The results give access to the ultralow interfacial tensions between the capillary bridge and the coexisting bulk phase. We demonstrate this with solutions of associative polymers and an aqueous mixture of gelatin and dextran, with interfacial tensions around 10 μN/m. The equilibrium nature of the capillary forces is attributed to the combination of a low interfacial tension and a microscopic confinement geometry, based on nucleation and growth arguments.

Interfaces are ubiquitous in soft matter and biological systems. The corresponding phase equilibria are often characterized by weak, tunable interactions and large length scales ξ. As a result, the interfacial tensions, $\gamma \propto k_B T / \xi^2$, are typically ultralow (i.e., $\ll 1$ mN m^{-1}).

Measurement of ultralow interfacial tensions is notoriously difficult. Many available techniques, such as drop shape [1] or interfacial profile analysis [2], rely on optical visualization. However, in weakly segregated and near-critical systems, the optical contrast between the phases is generally small. Moreover, density differences are also small, because of which it is difficult to obtain accurate information from drop shape analysis under normal gravity. To induce larger deformations, the spinning drop method is commonly used [3]. However, it was recently reported that the centrifugal field that is applied in this method, significantly affects the compositions of coexisting liquid phases. Demixed systems can even be brought into the one-phase regime [4].

The method that is presented in this Letter does not rely on optical contrast, density differences, or strong external fields. We use colloidal probe atomic force microscopy (CP-AFM), introduced independently by Ducker *et al.* [5] and Butt [6], to measure equilibrium forces originating from capillary, liquid bridges between two surfaces. We analyze the resulting force-separation profiles to extract ultralow interfacial tensions. In Fig. 1 we show a schematic representation of a capillary, liquid bridge between a sphere and a flat substrate, the characteristic configuration in the CP-AFM experiment.

When a homogeneous phase, in which one of the components is near its saturation point, is confined between two surfaces, a new phase can be formed by either condensation or evaporation. It is well known that, e.g., water condenses between hydrophilic surfaces in humid air [7]. Between hydrophobic surfaces at close separation, immersed in pure water, a capillary bridge of water vapor is formed, a process known as capillary evaporation or cavitation [8]. Capillary condensation is also reported for systems that show liquid-liquid coexistence, e.g., demixed

ternary polymer-solvent systems [9]. Because the curvature of the capillary bridge is negative with respect to the inner phase, a negative pressure difference is present across the interface, leading to an attractive force between the surfaces. In almost all experimental studies on capillary forces, nonequilibrium behavior is observed; i.e., there is hysteresis in the measured forces in a cycle of decreasing (approach) and increasing (retract) the separation between the surfaces.

In this Letter we consider aqueous solutions of telechelic associative polymers (hydrophilic polymers end-modified with hydrophobic tails); we use poly(ethylene oxide) (PEO) of various sizes that has been modified at both ends of the chain with C$_{12}$, C$_{14}$, C$_{16}$, or C$_{18}$ alkyl tails. In bulk, these systems weakly segregate into a dilute micellar phase (typically ~ 0.1 wt % polymer) and a phase relatively rich in polymer consisting of interacting micelles that are connected through bridges (typically ~ 3 wt %) [10], of which the latter wets the hydrophobic surfaces
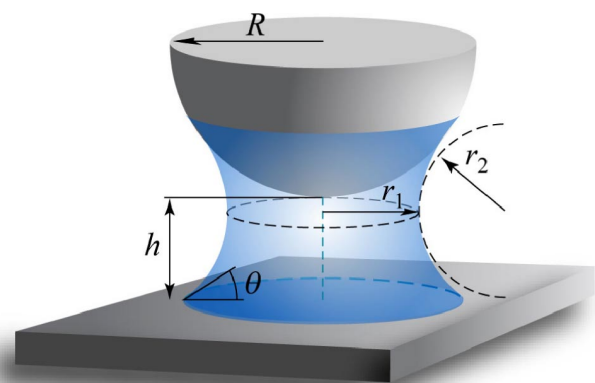

FIG. 1 (color online).   Artist's impression of a capillary bridge between a spherical probe with radius R and a flat substrate, where r_1 and r_2 are the principal radii of curvature at the minimal thickness of the bridge, θ is the contact angle at the three-phase boundary and h is the separation between the two surfaces.

104504-1

used in this study. The demixing is the result of an entropic attraction between the flowerlike micelles, due to bridge formation. Upon decreasing the distance between two hydrophobic surfaces immersed in a dilute, and homogeneous, solution of these polymers, we expect the formation of a condensed, polymer-rich capillary bridge.

For the CP-AFM measurements a silica sphere ($R = 3.0$ μm) is glued to the tip of a triangular AFM cantilever. The spherical probe, attached to the cantilever, and an oxidized silicon wafer (i.e., the flat substrate) are hydrophobized in the vapor of hexamethyl disilazane [11]. In a liquid cell, filled with aqueous solutions of the telechelic polymers, the distance between the hydrophobic probe particle and hydrophobic substrate (h) is varied. The deflection of the cantilever Δx at a given h can be converted into an interaction force F using Hooke's law $F = k \cdot \Delta x$, where k is the spring constant of the cantilever. We use cantilevers with a spring constant between 0.07 and 0.12 N m^{-1} as determined using the thermal fluctuations method of Hutter and Bechhoefer [12].

A typical force-distance curve is given in Fig. 2. It shows a long-ranged and weak attractive force, coming in at approximately 200 nm, and increasing in strength with decreasing h. The force curves we observe, share two remarkable features: (i) approach and retract curves coincide (no hysteresis), and (ii) there is no dependence on the approach and retract velocity (in the range of 100–1000 nm s^{-1}).

Various possible origins of this attraction can be considered, but most of them must be rejected. Depletion interactions are not a viable explanation, as we observe adsorption of the polymers onto these surfaces in optical reflectometry experiments and because the range of the attraction is many times larger than what is expected for
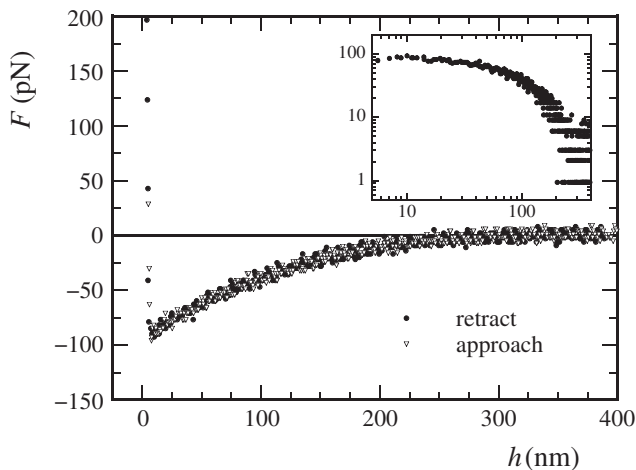

FIG. 2.   Interaction force, in pico newtons, between hydrophobic surfaces immersed in a 50 mg L^{-1} solution of C$_{18}$ end-modified PEO of 33 kg mol^{-1} (750 EO units, $M_W/M_N = 1.1$). Inset: absolute values of the force-distance curve plotted on a double logarithmic scale.

depletion interactions [13]. For polymeric, i.e., molecular, bridging one would expect the range of the interactions to depend on the chain length of the polymer, which is not found in our experiments at all. We find the same range of attraction (≈ 200 nm) for a C$_{12}$ end capped PEO of 5 kg mol^{-1} (110 EO-units) with a contour length of only 40 nm. For van der Waals interactions, the attractive force between a sphere and a flat surface should decay with h^{-2} [14]. The inset in Fig. 2 shows a force curve plotted on a double logarithmic scale, showing that we do not find the power-law behavior as expected for van der Waals interactions. We note that van der Waals forces are almost never found in AFM force measurements between silica surfaces in water, e.g., [15]. In the absence of polymers, the expected strong and long-ranged hydrophobic attraction [8] between the surfaces is observed (not shown). In the presence of associative polymer however, cavitation cannot occur because of the wetting layer that effectively changes the polarity of the surfaces. We therefore attribute the observed attractive forces to the action of a liquid bridge formed from a "dense" polymer phase.

The hysteresis-free nature of the force-distance measurements allows us to use equilibrium thermodynamics to analyze the results. The total capillary force can be divided into two components. The first contribution originates from the pressure difference across the interface, given by the Laplace equation: $\Delta P = \gamma(r_1^{-1} + r_2^{-1})$, where γ is the interfacial tension and r_1 and r_2 are the principal radii of curvature of the interface between the capillary bridge and the reservoir. The second contribution is due to the component of the interfacial tension normal to the substrate. To predict the capillary force as a function of distance for the sphere-plate geometry, one must find the optimal radii of curvature for given h. The solution should obey the constraint that the mean curvature $J = (r_1^{-1} + r_2^{-1})$ is constant for all positions along the hyperboloid shape, as the Laplace pressure must be homogeneous within the capillary bridge. A well-known approximate solution to this problem is $F \approx 4\pi R \gamma \cos\theta$ (see, e.g., [14]), where R is the radius of the spherical particle and θ is the contact angle at the three-phase boundary. The accuracy of this expression is, however, limited due to the many approximations in the derivation.

Instead, we prefer to use the more accurate solution of Willett and co-workers [16], who developed a solution to the Laplace equation for the sphere-plate geometry in the toroidal approximation, i.e., assuming that the shape of the capillary bridge matches the void in the center of a torus. The critical assumption in their work is that the volume of the liquid bridge V_b remains constant at all h, which could become less accurate when the systems are very close to their critical point. We numerically fit Willett's model to our experimental data, by inserting the known values for h and F and assuming a small contact angle ($\theta < 10°$), to find both V_b and the interfacial tension between the phase

relatively rich in polymer and the dilute micellar phase. In Fig. 3 we compare the experimental results with the best fit to the theoretical model for two different telechelic polymers. The agreement between model and experiment is good. The slight, yet systematic, deviations that are observed between the prediction by Willett *et al.* and our experimental data can be attributed to the nonexact nature of this theoretical description of equilibrium capillary forces, as implied by the approximations that were discussed above.

The interfacial tensions obtained for the associative polymer systems are plotted in Fig. 4 as a function of the number of carbon atoms n in the alkyl tails at both ends of the PEO chains. From the indicated error we can conclude that the accuracy of the present method is excellent.

Experimental results on the bulk phase behavior of these polymers indicate that decreasing the size of the hydrophobic tails, at a given PEO length and concentration, moves the weakly segregated system towards the critical point [10]. In Fig. 4 we see that γ decreases with decreasing n as expected. However, we must note that the experimentally accessible n range is too small to investigate the expected scaling behavior of the interfacial tension.

Often, capillary condensation phenomena are accompanied by hysteresis. It is therefore remarkable that we find no hysteresis in the force-distance curves, as shown in Fig. 2. This may be explained as follows: the formation of a capillary bridge consists of two steps, nucleation and growth. For heterogeneous nucleation, the energy barrier (ΔG^*) associated with the formation of a nucleus of critical dimensions, is proportional to γ [17]. The rate of nucleation is proportional to $\exp(-\Delta G^*/k_B T) \propto \exp(-\gamma A^*/k_B T)$, where A^* is the surface area of the critical nucleus. For systems with ultralow interfacial ten-

sions, nucleation is very fast, as the nucleation rate increases exponentially with decreasing interfacial tension. This explains why capillary condensation of water, or cavitation of water vapor, does gives rise to pronounced hysteresis [7,8], as the interfacial tension (between water and vapor) is a factor of 10^4 higher than that of the system considered here.

The rate of growth of the condensate is determined by the diffusion of polymer chains towards the capillary bridge. We can define a characteristic diffusion time (τ_D) as $\tau_D \approx L^2/D$, where D is the diffusion coefficient and L the mean diffusive path. From the Stokes-Einstein relation we estimate that the diffusion constant of a poly(ethylene oxide) chain of 750 EO units, which is the largest polymer considered in this Letter, is 4×10^{-11} m^2 s^{-1} in water at room temperature. The value of L depends strongly on the geometry of the experimental setup. From fitting the experimental data we have, in addition to the interfacial tension, also obtained the volume of the capillary bridge, which was consistently found to be in the order of 0.1 μm^3. Hence, the diameter of the capillary bridge is of the order of 0.1 μm at the onset of the capillary attraction ($h = 200$ nm). If we take 10 times this value as a rough estimate of the mean diffusive path (i.e., $L = 1$ μm), we find that $\tau_D = 25$ ms, whereas the experimental time scale is of the order of seconds. This may explain why transport towards the condensed phase is also not rate limiting, in this specific geometry.

Experiments in the surface force apparatus (SFA) on other demixed polymeric systems show pronounced nonequilibrium behavior, even when experimental time scales were many times larger than in our experiments [9]. In these experiments the interfacial tensions are of the same order of magnitude; hence the nucleation rate is expected to be similar to our case. However, the geometry in the
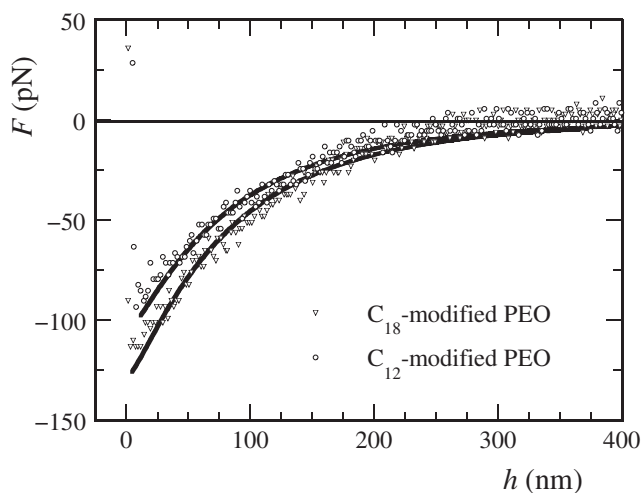

FIG. 3. Experimental force curves between hydrophobic surfaces in 50 mg L^{-1} aqueous solutions of C$_{12}$- and C$_{18}$-modified PEO of 33 kg mol^{-1} (750 EO units) (symbols), and curve fits to the model by Willett *et al.* [16] (drawn lines).
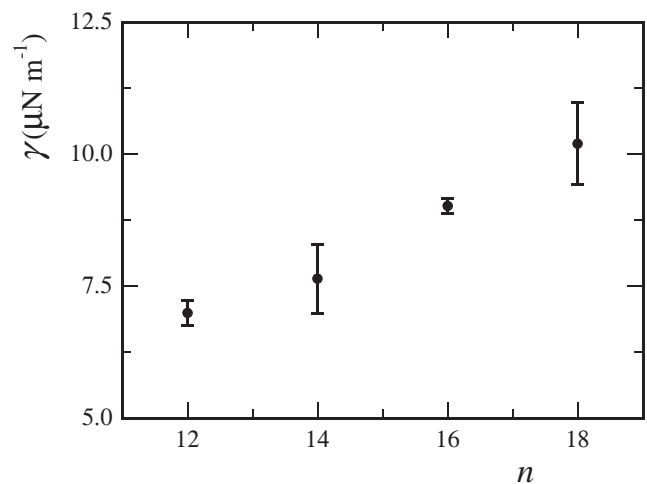

FIG. 4. Interfacial tensions versus the number of carbon atoms n in the hydrophobic alkyl tails at both ends of the PEO chain, for PEO of 33 kg mol^{-1} (750 EO units). Each point, with indicated error, is the average of at least 5 measurements.
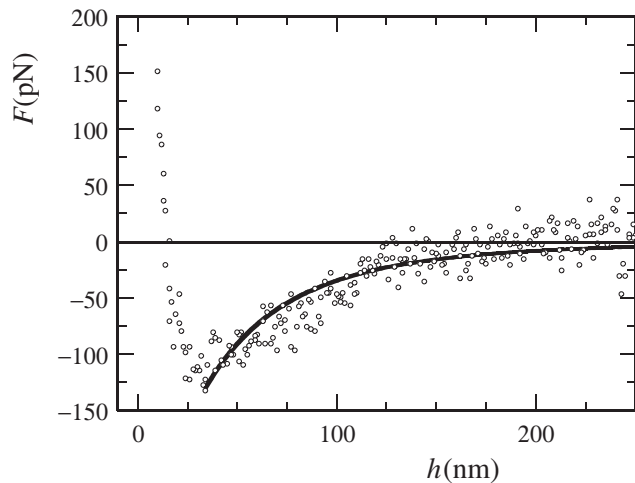
FIG. 5. Experimental force curve between hydrophilic surfaces in the dextran-rich phase of the demixed aqueous mixture of fish gelatin and dextran (overall polymer concentration of 9 wt %) (symbols), and curve fits to Willett's model (drawn line).

SFA, i.e., crossed cylinders with a curvature of the order of millimeters, gives a much larger characteristic time scale of diffusion. If the size of the capillary bridge is also of the order of millimeters in the SFA setup, τ_D increases from milliseconds in the CP-AFM experiment to several hours in the SFA geometry.

Clearly it is the specific combination of a microscopic geometry and a weakly segregated system that leads to the observation of equilibrium capillary forces. This implies that we should find equilibrium forces for many systems with ultralow interfacial tensions. As a further test we have therefore carried out measurements on a biphasic system of which the interfacial tension is reported in literature. We use a demixed mixture of fish gelatin and dextran in water, for which the interfacial tension has been reported to be 9 ± 3 $\mu\text{N}\,\text{m}^{-1}$ [18]. After formation of two macroscopic phases, one enriched in gelatin, the other in dextran, we fill the liquid cell of the AFM setup with the dextran-rich phase and repeat the experiment as described above with hydrophilic silica surfaces. It is known that the gelatin-enriched phase preferentially wets the silica surface (with $\theta = 0$) [19], we therefore expect condensation of a gelatin-rich phase between the silica sphere and substrate. The resulting force curve is shown in Fig. 5; the result is very similar to what is observed for the associative polymers. After fitting the data in the same manner as above, we find an interfacial tension of 15 ± 3 $\mu\text{N}\,\text{m}^{-1}$, which is in agreement with the value reported in literature.

For the gelatin-dextran system we observe a repulsion coming in at approximately 25 nm; for the associative polymers this did not show until $h = 5$ nm (Fig. 3). We must realize that the primary requirement for capillary condensation to occur is the presence of a wetting layer. For polymeric systems this entails adsorption of the poly-

mer, forming various structures at the solid surface. At small h, compression of these surface layers will result in a repulsion, that precedes the hard-wall repulsion at $h = 0$. For every experimental system the details of this phenomenon are different, as well as the time scales on which these effects are reversible. The short-ranged repulsion, found for both experimental systems, is thus fundamentally linked to the capillary condensation that causes the long-ranged attraction.

We conclude that we have measured equilibrium capillary forces between a microscopic spherical probe and a flat substrate. Through analysis of the resulting force-separation profiles we have directly obtained the ultralow interfacial tensions between the weakly segregated phases. A more detailed investigation of this subject matter is currently in preparation and will be published elsewhere.

*Joris.Sprakel@wur.nl
Also at: Dutch Polymer Institute (DPI), P.O. Box 902, 5600 AX Eindhoven, The Netherlands.
[1] J. N. Butler and B. H. Bloom, Surf. Sci. **4**, 1 (1966).
[2] D. G. A. L. Aarts, J. Phys. Chem. B **109**, 7407 (2005).
[3] J. L. Cayias, R. S. Schechter, and W. H. WadeAdv. Chem. Ser. **8**, 234 (1975).
[4] E. Scholten, L. M. C. Sagis, and E. van der Linden, Biomacromolecules **7**, 2224 (2006).
[5] W. A. Ducker, T. J. Senden, and R. M. Pashley, Nature (London) **353**, 239 (1991).
[6] H. J. Butt, Biophys. J. **60**, 1438 (1991).
[7] H. K. Christenson, J. Phys. Chem. **97**, 12 034 (1993).
[8] N. Bremond, M. Arora, C. D. Ohl, and D. Lohse, Phys. Rev. Lett. **96**, 224501 (2006).
[9] H. Wennerstroem, K. Thuresson, P. Linse, and E. Freyssingeas, Langmuir **14**, 5664 (1998).
[10] Q. T. Pham, W. B. Russel, J. C. Thibeault, and W. Lau, Macromolecules **32**, 2996 (1999).
[11] K. G. Marinova, D. Christova, S. Tcholakova, E. Efremov, and N. D. Denkov, Langmuir **21**, 11729 (2005).
[12] J. L. Hutter and J. Bechhoefer, Rev. Sci. Instrum. **64**, 1868 (1993).
[13] W. Knoben, N. A. M. Besseling, and M. A. Cohen Stuart, Phys. Rev. Lett. **97**, 068301 (2006).
[14] J. Israelachvili, *Intermolecular & Surface Forces* (Academic, London, 1985).
[15] W. A. Ducker, T. J. Senden, and R. M. Pashley, Langmuir **8**, 1831 (1992).
[16] C. D. Willett, M. J. Adams, S. A. Johnson, and J. P. K. Seville, Langmuir **16**, 9396 (2000).
[17] D. Turnbull, J. Chem. Phys. **18**, 198 (1950).
[18] E. Scholten, J. Sprakel, L. M. C. Sagis, and E. van der Linden, Biomacromolecules **7**, 339 (2006).
[19] R. H. Tromp and S. Lindhoud, Phys. Rev. E **74**, 031604 (2006).